Global statistical analysis of the protein homology network

C. Miccio*
Dipartimento di Fisica G.Occhialini, Università di Milano–Bicocca and INFN, Sezione di Milano, Piazza della Scienza 3 - I-20126 Milano, Italy

T. Rattei†
Department of Genome Oriented Bioinformatics, Technical University of Munich, Wissenschaftszentrum 5 Weihenstephan, 85350 Freising, Germany

(Dated: February 6, 2008)

The similarity between protein sequences is a directly and easly computed quantity from which to deduce information about their evolutionary distance and to detect homologous proteins. The *S*IMAP database – *S*imilarity Matrix of Proteins – provides a pre-computed similarity matrix covering the similarity space formed by about all publicly available amino acid sequences from public databases and completely sequenced genomes. From SIMAP we construct the protein homology network, where the proteins are the nodes and the links represent homology relationships. With more than 5 million nodes and about 70×10^9 edges it is the greatest protein homology network ever been builded. We describe the basic features and we perform a global statistical analysis of the network. Starting from the Smith-Waterman similarity score, we define for each edge a weight w to measure the similarity distance between two nodes. Keeping only edges with a weigth greater than a minimal $\bar{w}$, and by varying $\bar{w}$ we build a family of networks with different degree of similarity. We investigate the distribution of connected components (clusters) of the networks at different $\bar{w}$ and in particular we find a behaviour similar to a phase transition guided by the formation of a giant component. Moreover we study selected sequence features and protein domains of protein pairs that connect different clusters in the networks at different level of similarity. We observed specific, non-random distributions of the protein features and domains for proteins connecting clusters at certain weight intervals.

PACS numbers:

I. BACKGROUND

The number of known proteins is rapidly growing and the sequence of amino acids is, at the moment, the main source of information for many new proteins which still have unidentified functions. Protein sequence analysis, and more specifically, the analysis of similarities among protein sequences, is therefore the basis of studies trying to understand protein evolutionary processes or to detect unknown biological functions of new proteins. Proteins with similar sequences can be found in different organisms and in a single organism [12], [1]. By means of the degree of similarity obtained by a pairwise sequence comparison it is possible to deduce information about their evolutionary distance. Specifically, two proteins are homologous if they evolved from a common ancestral protein sequence and, in most cases, they have also the same, or very similar, biological function. Homology can be deduced from statistically significant sequence similarities. However, new sequences often have only weak similarities to known proteins, and single similarities search are insufficient to assign validated properties of characterized proteins to new sequences. Instead a graph formed by all-against-all comparisons of a large amount of protein-data could become useful. This is the case of **SIMAP** – *Similarity Matrix of Proteins* – a database containing the similarity space formed by almost all amino acid sequences, with nearly 5.5 million non-redundant protein sequences drawn from completely sequenced genomes and public database. Moreover, pre-calculated similarity space allows very rapid access to significant hits of interest and prevents time-consuming re-computation. The algorithm that precomputes the sequences similarities is based on the FASTA heuristic. First it compares low-complexity masked proteins using FASTA and then it recalculates the hits found using non-masked sequences and the Smith-Waterman algorithm. In both phases of the alignment process the BLOSUM50 amino acids substitution matrix is used. For each hit the Smith-Waterman score, the identity, the gapped identity, the overlap and the start and the stop coordinates of the alignment in both proteins are stored. For more details see [2].

Graphs formed by all-against-all sequence comparisons can be used to derive inheritance patterns of proteins, to reconstruct the evolutionary relationships between proteins and to classify them into protein families by looking for dense clusters disconnected from the rest of the network. To date, this approach has been carefully evaluated by case studies targeted at selected protein families [3], but a global analysis of the complete homology network formed by all publicly available proteins has not been published. The aim of this work is to analyze global and local properties of the graph forming the homology network.

*Electronic address: miccio@mib.infn.it
†Electronic address: t.rattei@wzw.tum.de

II. SIMAP GRAPH REPRESENTATION

The information contained in the Simap database can be reorganized by means of a weighted graph representation, $G(V, E, w)$, where V is the set of nodes, E the set of edges, and w a weight function on the edges: $w : E \to [0, 1]$. Each node, $\mathbf{a} \in V$, represents a protein sequence and each edge, $e = \{\mathbf{a}, \mathbf{b}\} \in E$ between two nodes $\mathbf{a}$, $\mathbf{b}$ represents the stored alignment between the respective protein sequences[13]. In this way an undirected weighted graph can be obtained, since the symmetry of the alignment procedure leads to undirected edges and the score of the alignment allows the assignment of a suitable weight to every edge. (Despite the possibility of making an alignment between a protein sequence and itself, self-edges are not considered). More specifically if $s(\mathbf{a}, \mathbf{b})$ is the Smith-Waterman (SW) optimal score obtained with the FASTA algorithm between sequence $\mathbf{a}$ and $\mathbf{b}$, a suitable weight $w(\mathbf{a}, \mathbf{b}) \in [0, 1]$ for the edge $e = \{\mathbf{a}, \mathbf{b}\}$ can be defined as follow:

$$w(\mathbf{a}, \mathbf{b}) = \frac{s(\mathbf{a}, \mathbf{b})}{\sqrt{s(\mathbf{a}, \mathbf{a})\ s(\mathbf{b}, \mathbf{b})}}, \qquad (1)$$

From $w(\mathbf{a}, \mathbf{b})$ one could define a distance function as $d(\mathbf{a}, \mathbf{b}) = 1 - w(\mathbf{a}, \mathbf{b})$, whose values are in $[0, 1]$ as distance function usually defined on linear spaces. d should satisfy positivity, null and simmetry properties for all pairs of sequence proteins and also the triangular inequality which is fully satisfied for the BLOSUM50 matrix.

III. POLISHING PROCEDURE

Strictly speaking, the set of all protein sequences of the Simap database is not a good space over which to define the distance measure d. There are, in fact, 1538 pairs of sequences that have distance equal to zero, although they are classified with a different sequence id. However, they differ only in the presence of one or two 'X' in their amino acid sequence annotation, where 'X' is the standard symbol for an unknown amino acid residue in a protein sequence. It is therefore natural to decide to knock out, for each of these pairs of sequences, the one that has the 'X' in the sequence; this procedure entails the removal, in the graph representation, of all edges connected to the removed nodes. Another improvment for database consistency is the checking of symmetry of all edges: every time, a direct edge is found, the inverse relation, if absent, is added.

As a final result of these manipulations, a graph with $V = 5,489,907$ nodes and $E = 69,500,722,050$ edges can be constructed.

Over the polished Simap protein sequences space the distance $d = 1 - w(\mathbf{a}, \mathbf{b})$ fails the triangular inequality over few cases (around $\approx 0.2\%$ of triangles). However redefining, for istance,

$$d(\mathbf{a}, \mathbf{b}) = \sqrt{1 - w(\mathbf{a}, \mathbf{b})}, \qquad (2)$$

we have that the triangle inequality is satisfied for all triples of linked proteins and (2) has all properties required for a *distance measure*.

IV. CHARACTERIZATION OF SIMAP PROTEIN SPACE

In the Simap database, protein sequences come from 104,560 different species. There are, in particular, 3 species (*Homo sapiens*, *Arabidopsis thaliana*, *Rice plants*) with more than 100,000 protein sequences and 72 with more than 10,000.

kingdoms		*number of species*
bacteria		11,130
viruses	viruses	13,708
	phages	923
plants		31,232
animalia	invertebrates	25,951
	vertebrates	19,341
	(rodents)	(1,474)
	(mammals)	(1,854)
	(primates)	(393)
environmental samples		1,453
synthetic		822

TABLE I: Number of species for each kingdom.

A coarse subdivision of all species is shown in Table I; it separates species in five (non-standard) main kingdoms: bacteria, viruses, plants, invertebrates (animalia) and vertebrates (animalia). The classification reveals the presence of very many different animalia species, but only eight of these species are present with their complete genome (the other animalia proteins were imported from multiple species databases). Figure 1 shows the protein distribution for each kingdom. There is also a high number (546,439) of unassigned protein sequences.[14].

A. Length and self-similarity distribution

The protein sequences space is characterized by the length distribution shown in Figure 2a and in Figure 2b we give the length distributions for sequences belonging to bacteria, viruses, plants, vertebrates and invertebrates.

The *self-similarity score* 's distribution of protein sequence appears in Figure 3. The self-similarity scores distribution is well reproduced by a mixture of normal distributions, one for each length entry. The self-similarity score $s(\mathbf{a}, \mathbf{a})$ of a protein sequence of length

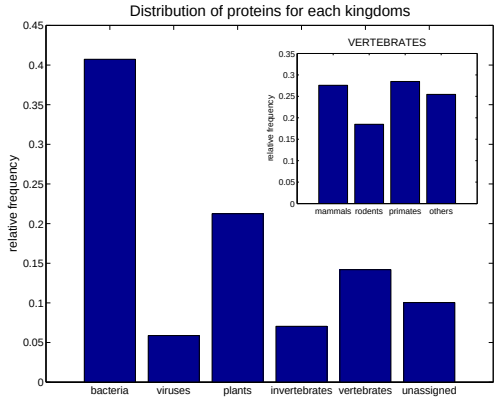

FIG. 1: Distribution of proteins for each kingdom. The little graph shows the distribution within vertebrates.

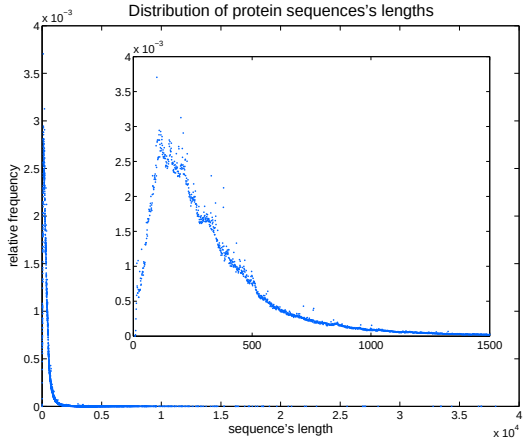

(a)

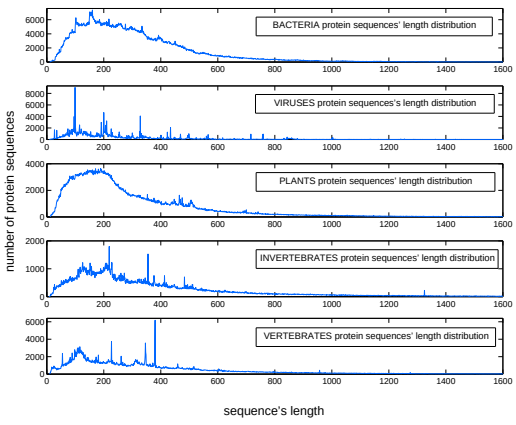

(b)

FIG. 2: (a) Distribution of protein sequences' lengths. In the inner boxe an enlargement of the distribution is shown. (b) Length distributions of protein sequences which belong to *bacteria* ($\langle l\rangle = 316.9$, $l_{max} = 36805$), *viruses* ($\langle l\rangle = 273.9$,$l_{max} = 7312$), *plants* ($\langle l\rangle = 314.5$, $l_{max} = 20925$), *invertebrated* ($\langle l\rangle = 416.1$, $l_{max} = 23015$), *vertebrated* ($\langle l\rangle = 397.1$, $l_{max} = 38031$).

l, can be thougth as a sum of l i.i.d. random variables, i.e. a sum of the self-similarities scores of random amino acids. Knowing the amino acids background probabilities[15] p_a and the diagonal values of the BLOSUM50 score matrix, B_{aa}, the self-similarity score of a random amino acid will follow a normal distribution with mean $\langle s\rangle = \sum_a p_a B_{aa}$ (≈ 6.727) and variance $\sigma = \sqrt{\sum_a p_a B_{aa}^2 - \langle s\rangle^2}$ (≈ 2.067). Self-similarity scores of random amino acid sequences of length l will have a normal distribution $g(l,s)$ with mean $l\,\langle s\rangle$ and variance $\sqrt{l\,\sigma^2}$. Finally, the self-similarity scores distribution is well approximated by the sum $\sum_l g(l,s)f(l)$, where $f(l)$ is the observed length distribution, Figure 4.

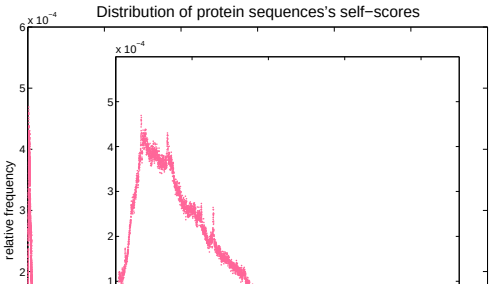

FIG. 3: Distribution of protein sequences' self-scores. In the inner boxe an enlargement of the distribution is shown.

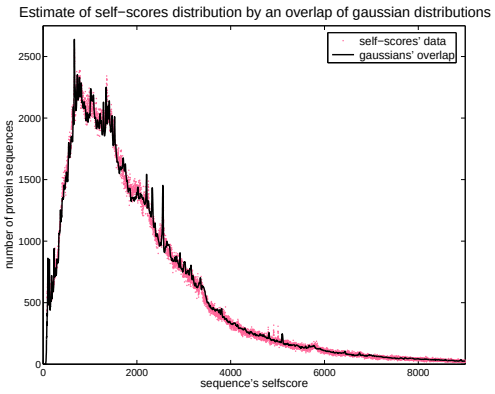

FIG. 4: Distribution of protein sequences' self-scores and the curve obtained by an overlap of normal distributions opportunely wighted by the protein sequences's length distribution are compared.

B. Pairwise similarity distribution

The SW optimum similarity scores distribution obtained from all FASTA sequence alignments present a homogeneous cutoff equal to 80, used for storing hits

in Simap database. It was chosen independently of the query and database length, but as an optimal compromise between sensitivity and possibility to store an accessible number of hits, because of the high number of protein sequences.

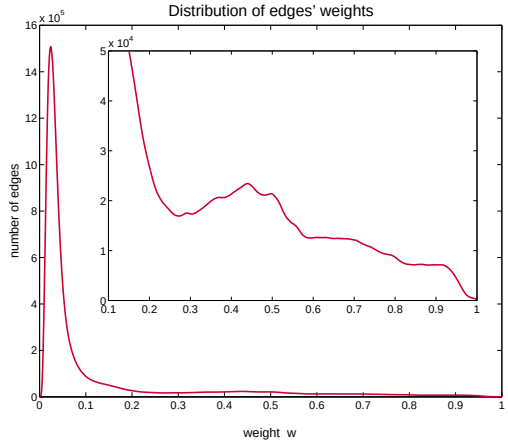

(a)

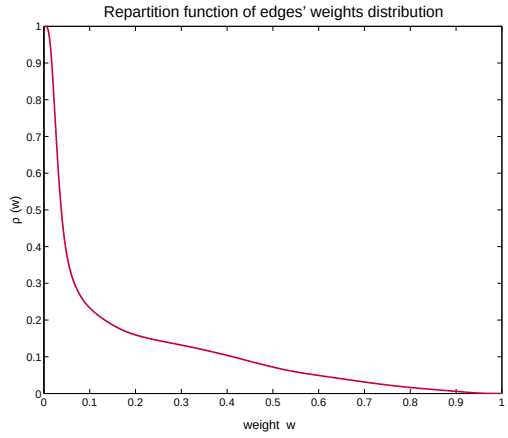

(b)

FIG. 5: (a) Distribution of edges' weights w. In the inner box is shown an enlargement of the distribution tail. (b) Repartition function edges' weights distribution.

In Figure 5a the distribution of weights w is shown, and in Figure 5b the corresponding repartition distribution $\rho(w)$. The values of $\rho(w) \in [0,1]$ represent the fractions of edges which have weight greater or equal to w. From them we see that the major part of the edges (about 80% of the total number of edges) has a very low value of w (≤ 0.2).

C. Coordination and cluster distribution

Weights w can be used as a parameter to define a collection of graphs. For a fixed value of $w = \bar{w}$ (or a value of $d = \bar{d} = \sqrt{1-\bar{w}}$), a graph is built keeping only edges with $w > \bar{w}$ ($d \leq \bar{d}$). For high values of $\bar{w}$, i.e. at small distances, nodes are linked if, and only if, the corresponding protein sequences have a high degree of similarity; then it is reasonable to expect graphs with many small connected components. By decreasing $\bar{w}$' values, in other words by also linking proteins having a lower degree of similarity, graphs with larger connected components are expected. The graph obtained by considering all possible edges (by fixing $\bar{w} = 0$) is not the complete graph, due to the cutoff on the score alignment (there are about 0.1% of edges of the corresponding complete graph).

We have built graphs for values of w equal to 0.975, 0.95, 0.925, 0.9, 0.875, 0.85, 0.825, 0.8, 0.775, 0.75, 0.725, 0.7, 0.675, 0.65, 0.625, 0.6, 0.575, 0.55, 0.525, 0.5, 0.475, 0.45, 0.425, 0.4 0.375, 0.35, 0.325, 0.3, 0.275, 0.25, 0.225, 0.2, 0.175, 0.15, 0.125; for each of these values the set of the protein sequences splits into clusters, i.e. isolated connected components. Linking proteins that have a greater and greater distance from each other (decresing $\bar{w}$), clusters merge to form larger clusters, the number of isolated proteins and the number of components with a very small size decreases, while the number of clusters of medium and large size increases.

Measuring the (not normalized) cluster distribution, we find that, for each fixed values of $\bar{w}$, the number of clusters $n_{\bar{w}}(s)$ of size s follows, in a specific size range, a power law behaviour, $n_{\bar{w}}(s) \sim s^{-\sigma(\bar{w})}$. Fitted values of $\sigma(\bar{w})$ and fitting size ranges are reported in Table II and a log-log plot of size distribution $n_{\bar{w}}(s)$, for three different values of $\bar{w}$ is shown in Figure 6(a). Also the (not normalized) coordination degree distribution $f_{\bar{w}}(z)$ follows a power law distribution, $f_{\bar{w}}(z) \sim z^{-\alpha(\bar{w})}$, for each values of $\bar{w}$. A log-log plot of coordination degree distribution $f_{\bar{w}}(z)$, for three different values of $\bar{w}$ is shown in Figure 6(b). Fitted values of $\alpha(\bar{w})$ and fitting coordination degree's ranges are reported in Table III.

$\bar{w}$	σ	component size range	correlation coefficient
0.95	2.70	10 – 60	−0.995
0.90	2.70	10 – 60	−0.996
0.85	2.69	10 – 60	−0.994
0.80	2.62	10 – 80	−0.996
0.75	2.52	10 – 80	−0.996
0.70	2.40	10 – 80	−0.996
0.65	2.32	10 – 100	−0.997
0.60	2.21	10 – 100	−0.996
0.55	2.17	10 – 100	−0.996
0.50	2.07	10 – 100	−0.997
0.45	2.01	10 – 100	−0.997
0.40	2.00	10 – 100	−0.996
0.35	1.98	10 – 100	−0.997
0.30	1.98	10 – 100	−0.997
0.25	2.01	10 – 100	−0.996

TABLE II: Fitting values of exponent σ of the power law distribution of connected components for selected values of $\bar{w}$. For each fitting the size range and its correlation coefficient are reported.

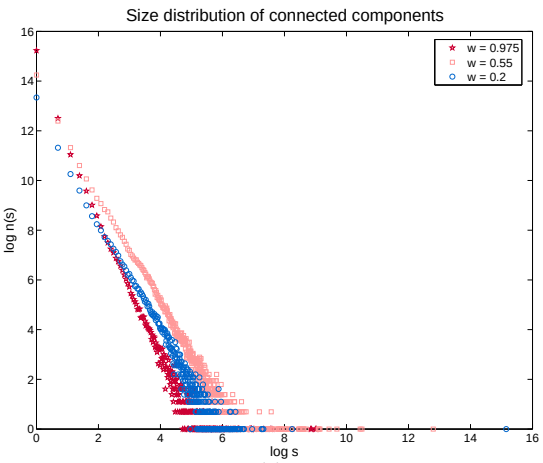

(a)

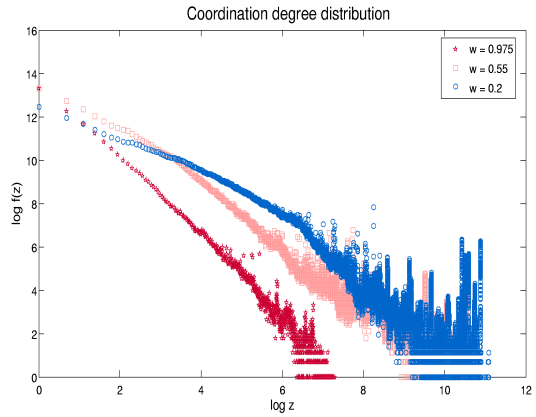

(b)

FIG. 6: (a) Distribution of size of connected components of the protein sequences graph built at $\bar{w} = 0.975$ (red curve), $\bar{w} = 0.75$ (pink curve) and $\bar{w} = 0.4$ (blue curve). It is evident that as the $\bar{w}$ value decrease the number of connected components with small size decreases and the starting region of the power law behaviour shifts to higher values of size. (b) Distribution of coordination degree of the protein sequences graph built at $\bar{w} = 0.975$ (red curve), $\bar{w} = 0.75$ (pink curve) and $\bar{w} = 0.4$ (blue curve). As the $\bar{w}$ value decrease the number of nodes with coordination degree decreases and the starting region of the power law behaviour shifts to higher values of coordination degree.

$\bar{w}$	$\langle z \rangle$	max z	α	coordination degree range	correlation coefficient
0.95	14.4	5735	1.59	25 – 100	−0.990
			1.46	100 – 500	−0.953
0.90	73.1	10794	1.58	25 – 100	−0.988
			1.51	100 – 500	−0.939
0.85	138.3	16500	1.68	25 – 100	−0.993
			1.42	100 – 800	−0.964
0.80	207.2	23726	1.73	25 – 100	−0.994
			1.29	100 – 800	−0.941
0.75	294.0	33265	1.79	25 – 100	−0.997
			1.22	100 – 1000	−0.956
0.70	395.3	35202	1.74	25 – 100	−0.996
			1.28	100 – 1000	−0.946
0.65	507.8	36333	1.71	25 – 100	−0.998
			1.39	100 – 1000	−0.950
0.60	622.3	37729	1.63	25 – 100	−0.999
			1.32	100 – 1500	−0.930
0.55	745.3	41871	1.54	25 – 100	−0.998
			1.44	100 – 1500	−0.927
0.50	911.7	49895	1.44	25 – 100	−0.998
			1.56	100 – 2000	−0.944
0.45	1108.1	51309	1.38	25 – 100	−0.998
			1.62	100 – 2000	−0.951
0.40	1314.2	51956	1.28	25 – 100	−0.998
			1.67	100 – 2500	−0.946
0.35	1501.9	52513	1.19	25 – 100	−0.998
			1.72	100 – 2500	−0.961
0.30	1668.9	60722	1.08	25 – 100	−0.997
			1.74	100 – 3000	−0.969
0.25	1826.2	64781	0.97	25 – 100	−0.997
			1.78	100 – 3000	−0.969

TABLE III: Fitting values of exponent α of the power law distribution of coordination degree for selected values of $\bar{w}$. We compute two linear fittings different in the choice of fitting range of coordination degree. For each fitting the range of coordination degree and its correlation coefficient are reported. In the second column the average degree is shown; the third column gives the maximum value of the coordination degree.

V. COMPARISON WITH GENERALIZED RANDOM GRAPHS

It would be interesting to compare these behaviours with that of a model of random graphs. It is well known that, in the classical model, random graphs (where every pair of nodes is chosen to be an edge with probability p, as introducede by Erdös-Rényi [4]), have the same expected coordination degree at every node, so they are characterized by a poissonian coordination degree distribution with mean value $\langle z \rangle \sim pV$. Futhermore, as soon as $\langle z \rangle$ assume a value greater than 1, a giant connected component appears, that is a component whose size is much greater than the size of all other components, and that represents an important fraction of all graph's nodes.

A better theorical comparison model could be represented by generalized random graphs endowed with a specific degree-distribution. These can be generated via the Monte-Carlo algorithm (following the work in [5] of Burda et al.). In particular, starting from a random graph of V nodes and E edges, making local graph transformations which leave the number of nodes and the number of edges constant and accepting them with a probability which depends on the desired equilibrium degree distribution (Metropolis algorithm), we have generated a collection of random graphs with the same coordination degree distribution and the same average degree as some of our protein sequences graphs.

For each of them we observe a fundamentally different distribution of connected components in the protein sequences graphs and in the random graphs. In the latter model the power law behaviour is absent, while there is a always a dominant giant connected component, much larger than the many other small components, whose size distribution decreases exponentially (See Figure 7).

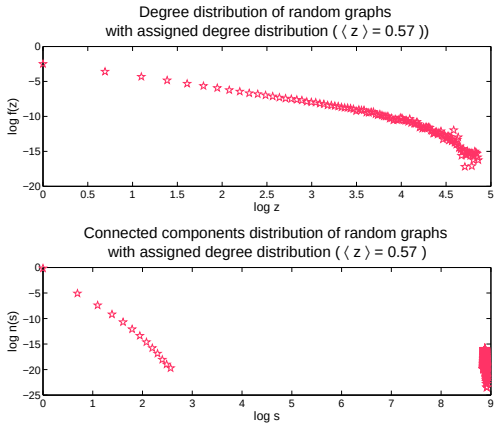

FIG. 7: Top: coordination degree distribution of the collection of random graphs generated via Monte-Carlo algorithm fixing the equilibrium degree distribution equal to that one observed in the protein sequences graph at $\bar{w} = 0.99$ and fixing the average degree equal to $\langle z \rangle = 0.57$. Bottom: size distribution of connected components of the random graphs.

By comparison, in the Simap protein sequences space the coordination degree distribution $f_{\bar{w}}(z)$ and the connected component distribution $n_{\bar{w}}(s)$ are strongly correlated. The former, for example, can be reproduced quite well by means of $n_{\bar{w}}(s)$. Let the index i label all connected components and let us consider all possible edges between nodes belonging to a connected components of size s_i; then the cluster would be a complete subgraph and all its s_i nodes would have coordination degree equal to $z_i = s_i - 1$. If this were true for all connected components then all clusters would be complete subgraphs and we would expect a coordination degree distribution equal to $f_{\bar{w}}(z) \sim (s\ n_{\bar{w}}(s))|_{s=z+1}$. In our graphs, although complete connected components are present, the majority of clusters have only a high average degree distribution, not equal to its size minus one, as in complete graphs. However let's consider a component with size s_i and a number of edges equal to m_i; the quantity $\Delta_i = \frac{2m_i}{s_i(s_i-1)}$ represents the fraction of edges that are present in the i-th component respect to the number of edges that would be present if the component were a complete subgraph (i.e. $s_i(s_i-1)/2$). Introducing Δ_i as a measure of edges' density for each component we can approximate the coordination degree distribution $f_{\bar{w}}(z)$ by means of the size connected component distribution $n_{\bar{w}}(s)$ too. Specifically we find that the coordination degree distribution behaves like $f_{\bar{w}}(z) \sim \bar{\Delta}(z+1)\ (z+1)\ n_{\bar{w}}(z+1)$, where $\bar{\Delta}(s)$ is the edges' density averaged over all components of size s: $\bar{\Delta}(s) = \frac{\sum_i \delta_{s_i,s}\Delta_i}{\sum_i \delta_{s_i,s}}$. Figure 8 shows both the observed degree distribtution and the approximated degree distribution obtained by means of $n(s)$ of the graph at $\bar{w} = 0.95$.

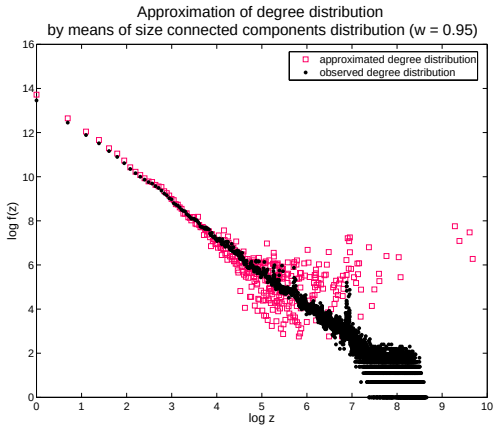

FIG. 8: Observed degree distribution (black curve) and the approximated degree distribution (red curve) obtained by means of $n(s)$ of the graph at $\bar{w} = 0.95$.

VI. GIANT COMPONENT

An interesting phenomenon occurs when $\bar{w}$ value decrease; we see the formation of the giant component. In Figure 9a the behaviour of the fraction of nodes belonging to the largest component is shown.

Starting from approximately $\bar{w} \sim 0.65$ the largest component begins to expand its size capturing a lot of smaller components. Furthermore the components which are disconnetted at $\bar{w} \sim 0.675$ and which go to form the giant component at $\bar{w} \sim 0.65$ are samples of many different sizes, from small components to very big components. This phenomenon becomes more and more evident for lower values of $\bar{w}$, when the coordination degree distribution of the giant component follows a power law scaling. This is evident also from Figure 6(b), where we plot the distribution of the coordination degree for the whole set of proteins. The exponent $\alpha(\bar{w})$ of the power law behavior $f_{\bar{w}}(z) \sim z^{-\alpha(\bar{w})}$ varies slightly between the regions corresponding to small values of the coordination degree z and to large values of z. Clearly when a giant component exists, the region with large z is largely determined by the giant component itself. In Table III we report the fitting values of the exponent $\alpha(\bar{w})$ computed in two regions with small and large values of z. As we decrease the value of $\bar{w}$, the two fitting values of $\alpha(\bar{w})$ become more and more divergent. In fact, since the largest component is growing, the tail of the distribution $f_{\bar{w}}(z)$ becomes more and more important and assumes a power law behavior characterized by a different exponent.

A significant fact goes with the rapid size increase of the largest component. In Table IV we show, for each $\bar{w}$, the fraction of different kingdoms and the number of

$\bar{w}$	$\bar{d}$	size	bacteria	viruses	plants	invertebrates	vertebrates	number of different species
0.975	0.1581	8322	0.000	1.000	0.000	0.000	0.000	4
0.950	0.2236	15955	0.000	1.000	0.000	0.000	0.000	4
0.925	0.2739	47687	0.000	1.000	0.000	0.000	0.000	10
0.900	0.3162	50729	0.000	1.000	0.000	0.000	0.000	14
0.875	0.3536	51028	0.000	1.000	0.000	0.000	0.000	14
0.850	0.3873	51405	0.000	1.000	0.000	0.000	0.000	14
0.825	0.4183	51969	0.000	1.000	0.000	0.000	0.000	29
0.800	0.4472	52097	0.000	1.000	0.000	0.000	0.000	29
0.775	0.4743	52881	0.000	1.000	0.000	0.000	0.000	29
0.750	0.5000	63003	0.000	1.000	0.000	0.000	0.000	60
0.725	0.5244	118777	0.000	1.000	0.000	0.000	0.000	67
0.700	0.5477	120974	0.000	0.999	0.000	0.000	0.000	106
0.675	0.5701	145278	0.002	0.997	0.000	0.000	0.000	302
0.650	0.5916	224310	0.002	0.749	0.001	0.000	0.248	988
0.625	0.6124	272426	0.014	0.662	0.010	0.007	0.306	4384
0.600	0.6325	297280	0.028	0.643	0.015	0.011	0.303	7854
0.575	0.6519	318472	0.032	0.613	0.027	0.015	0.313	9668
0.550	0.6708	362379	0.047	0.554	0.035	0.024	0.341	11437
0.525	0.6892	404788	0.049	0.526	0.047	0.029	0.349	15593
0.500	0.7071	450072	0.065	0.482	0.055	0.033	0.365	16272
0.475	0.7246	584371	0.084	0.379	0.151	0.037	0.349	20957
0.450	0.7416	718286	0.114	0.312	0.194	0.041	0.340	35346
0.425	0.7583	975629	0.151	0.229	0.184	0.095	0.341	68338
0.400	0.7746	1202753	0.181	0.188	0.209	0.096	0.326	76230
0.375	0.7906	1435734	0.210	0.160	0.224	0.093	0.312	77970
0.350	0.8062	1739772	0.254	0.133	0.236	0.087	0.291	80100
0.325	0.8216	2059217	0.288	0.117	0.239	0.083	0.273	82714
0.300	0.8367	2383804	0.316	0.102	0.244	0.080	0.258	84953
0.275	0.8515	2728214	0.350	0.090	0.243	0.078	0.239	86151
0.250	0.8660	3071192	0.374	0.083	0.240	0.076	0.226	90357
0.225	0.8803	3420697	0.396	0.078	0.239	0.074	0.213	94210
0.200	0.8944	3807556	0.416	0.076	0.237	0.073	0.199	101358
0.175	0.9083	4210208	0.432	0.074	0.234	0.072	0.188	102774
0.150	0.9220	4651704	0.446	0.072	0.233	0.073	0.177	103831
0.125	0.9354	5049016	0.455	0.069	0.235	0.073	0.167	104227

TABLE IV: For each fixed values of $barw$, we computed the percentage of proteins, among those belonging to the largest component, that come from the five kingdoms.

different species which appear in the largest connected component. Down to around $\bar{w} = 0.675$ only proteins coming from viruses belong to the largest component and, moreover this largest cluster has not yet become giant with respect to smaller clusters. For $\bar{w} \lesssim 0.675$ the formation of a giant component begins, and simultaneously all kinds of kingdoms enter in the species composition of the giant cluster. This is also evident from Figure 9b, where we plot the fraction of the number of species belonging to the largest component. This ratio increases rapidly around the same value of $\bar{w}$. These processes continue for lower values of $\bar{w}$, with the giant component including more and more proteins belonging to many different species, and the ratio for each kingdom tends to become the same as that of the whole database. Furthermore around $\bar{w} \simeq 0.475$ there is a very sharp increase both in the dimension of the giant component and especially in the number of species present in it, as it is evident from Figures 9a and 9b.

The processes just described may indicate the presence of a phase transition: we have two different phases, one for large values of $\bar{w}$, characterized by the presence of clusters with similar dimensions and with the largest one composed especially of viruses, and the second phase characterized by the presence of a giant component composed of different species alongside other small little clusters. We note however that the phase transition is not sharp, but the changes in the dimension and composition of the largest component are spread in a range $0.475 < \bar{w} < 0.675$. We also note that the plot in Figure 9b has a very rapid increase for $w \sim 0.475$.

In Table V, for each $\bar{w}$, it can be seen how different kingdoms are distributed in connected components. In particular we count the number of components, whose size is greater than 90 and record the percentage of clusters whose proteins come from species of only one kingdom, only from a pair of kingdoms, etc., up to the percentage of connected components which contain pro-

$\bar{w}$	0.95	0.90	0.85	0.80	0.75	0.70	0.65	0.60	0.55	0.50	0.45	0.35	0.25	0.15
bacteria	9.6	12.2	14.2	17.2	21.9	22.6	23.6	23.8	23.9	25.1	25.8	29.0	35.6	57.0
viruses	32.7	31.4	24.3	17.6	11.4	7.4	5.2	3.8	2.9	2.7	2.4	2.7	4.2	7.5
plants	9.3	10.8	11.4	9.4	8.3	7.3	7.6	7.8	7.7	7.5	7.5	6.2	4.0	0.0
invertebrates	11.6	8.9	7.4	5.8	3.6	3.2	2.5	2.0	1.6	1.5	1.2	1.4	1.3	1.1
vertebrates	22.9	23.0	25.4	25.7	25.6	25.9	23.6	20.0	17.1	13.0	10.2	5.2	2.8	1.1
bac-vir	2.7	2.2	2.1	2.1	1.6	1.6	1.4	1.0	1.0	1.1	1.0	1.7	2.4	3.2
bac-pla	1.6	1.8	2.8	2.9	3.5	4.5	5.9	7.0	8.5	8.9	9.1	10.8	11.3	18.3
bac-inv	0.5	0.4	0.7	0.7	0.8	0.9	1.3	1.7	2.1	2.1	2.0	2.6	3.0	1.1
bac-ver	1.8	2.0	2.4	2.3	1.9	1.9	1.8	1.6	1.5	1.5	1.3	1.1	1.1	1.1
vir-pla	0.2	0.1	0.2	0.4	0.3	0.4	0.3	0.3	0.2	0.2	0.2	0.2	0.5	0.0
vir-inv	0.0	0.0	0.0	0.0	0.0	0.0	0.0	0.0	0.0	0.0	0.0	0.0	0.0	0.0
vir-ver	0.2	0.5	0.7	0.8	0.9	0.7	0.6	0.4	0.3	0.2	0.1	0.2	0.1	0.0
pla-inv	0.9	0.0	0.0	0.0	0.0	0.2	0.1	0.1	0.1	0.2	0.3	0.2	0.5	0.0
pla-ver	0.5	0.9	0.8	1.1	1.3	1.0	1.1	1.2	1.2	1.0	0.9	1.3	1.7	1.1
inv-ver	0.5	1.1	2.6	4.5	7.0	8.4	9.2	10.3	10.9	11.2	11.0	9.0	5.5	0.0
bac-vir-pla	0.0	0.4	0.3	0.5	0.3	0.3	0.4	0.2	0.2	0.2	0.4	0.4	0.7	1.1
bac-vir-inv	0.0	0.0	0.0	0.0	0.0	0.0	0.0	0.0	0.1	0.0	0.1	0.1	0.3	1.1
bac-vir-ver	0.2	0.1	0.0	0.0	0.0	0.1	0.1	0.1	0.1	0.1	0.2	0.2	0.2	0.0
bac-pla-inv	0.0	0.0	0.1	0.2	0.5	0.6	0.8	0.9	1.3	2.0	2.3	2.4	3.1	1.1
bac-pla-ver	0.0	0.1	0.0	0.0	0.1	0.3	0.6	0.6	0.9	1.0	1.3	1.7	1.4	0.0
bac-inv-ver	0.0	0.0	0.1	0.3	0.4	0.4	0.4	0.9	0.8	0.9	0.9	1.0	0.8	1.1
vir-pla-inv	0.0	0.0	0.0	0.0	0.0	0.0	0.0	0.0	0.0	0.0	0.0	0.0	0.0	0.0
vir-pla-ver	0.0	0.0	0.0	0.0	0.1	0.1	0.1	0.0	0.0	0.0	0.0	0.0	0.0	0.0
vir-inv-ver	0.0	0.0	0.1	0.2	0.1	0.2	0.3	0.2	0.2	0.2	0.2	0.1	0.1	0.0
pla-inv-ver	0.9	1.4	1.8	5.5	7.3	8.4	9.4	11.0	11.3	12.0	12.4	13.4	11.7	0.0
bac-vir-pla-inv	0.0	0.0	0.0	0.0	0.0	0.0	0.0	0.1	0.1	0.1	0.1	0.2	0.0	0.0
bac-vir-pla-ver	0.0	0.0	0.1	0.1	0.1	0.1	0.2	0.1	0.1	0.1	0.1	0.1	0.1	0.0
bac-vir-inv-ver	0.0	0.0	0.0	0.0	0.0	0.0	0.0	0.0	0.0	0.0	0.0	0.1	0.1	0.0
bac-pla-inv-ver	0.2	0.1	0.4	0.7	1.0	2.1	2.5	3.8	5.1	6.4	8.0	7.6	6.7	0.0
vir-pla-inv-ver	0.0	0.1	0.0	0.0	0.1	0.1	0.2	0.3	0.3	0.3	0.2	0.2	0.1	1.1
bac-vir-pla-inv-ver	0.0	0.0	0.1	0.1	0.1	0.2	0.2	0.1	0.2	0.3	0.5	0.7	0.4	1.1

TABLE V: Spread of species in connected components. Each value indicates the percentage of clusters, calculated on clusters having size greater than 90, composed by proteins coming from only one kingdom, only from a pair of kingdoms, etc., up to the percentage of clusters composed by proteins of all kingdoms.

teins of all kingdoms. For high values of $\bar{w}$ the majority of clusters are made up of proteins belonging to only one kingdom, in particular the kingdom of viruses; clusters with proteins of different kingdoms are very scarce. As expected, as $\bar{w}$ decreases, the percentage of clusters belonging to only one kingdom decreases in favor of clusters of mixed kingdom composition.

It is interesting to note that the virus kingdom has a very low tendency to cluster with the other kingdoms, in particular with plants and animalia. Furthermore, for no values of $\bar{w}$ do we see the formation of components (of size greater than 90) with proteins coming from viruses and invertebrates, and from viruses, plants and invertebrates. Virus proteins cluster mainly with bacterial proteins. In addition we observe that bacterial proteins cluster mainly with plant proteins and vice versa. Moreover, although plant proteins cluster infrequently with invertebrates and with vertebrates, there are many more clusters consisting simultaneously of plant, invertebrate and vertebrate proteins. Finally we note that at the lowest value of $\bar{w}$, the majority of components which are not included in the giant component are clusters consisting of bacterial proteins, of bacterial and plant proteins and of virus proteins.

VII. ANALYSIS OF THE PROTEINS THAT CONNECT CLUSTERS

Protein pairs that connect clusters in the different weight intervals are of special interest as they harbor the most conserved sequence regions that are shared by the interconnected clusters. We want to know if certain sequence features and protein domains are enriched in these proteins compared to the complete proteome. Therefore we have calculated for all protein contained in SIMAP some sequence features: *length*, *isoelectric point* (using the EMBOSS sequence analysis package [6]), *low complexity content* (using the program seg [7]) and the number of *predicted transmembrane segments* (using the program TMHMM [8]). Additionally, in order to derive functional information for all proteins, we have predicted *signal peptides* (using SignalP 3.0 [9]), *localization signals* (using TargetP 1.1[10]) and *protein domains* (using the databases PFAM, TIGRFAM, PANTHER, SUPERFAMILY, SMART and PIRSF from InterPro 12.1 [11]) for

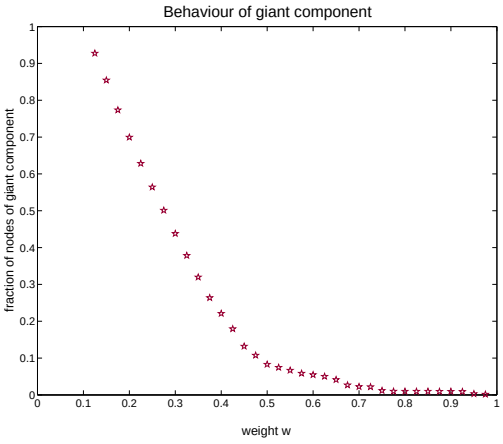

(a)

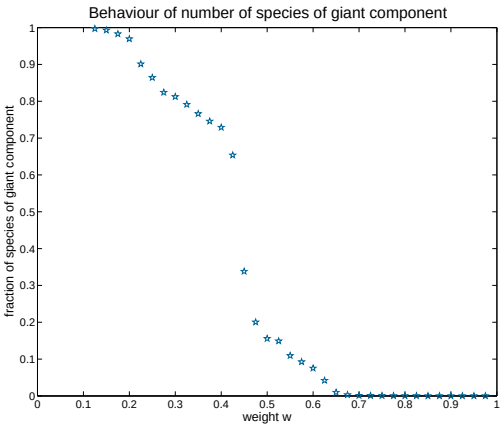

(b)

FIG. 9: (a) Fraction of nodes belonging to the largest cluster for each value of $\bar{w}$. (b) Fraction of species present in the largest cluster for each value of $\bar{w}$.

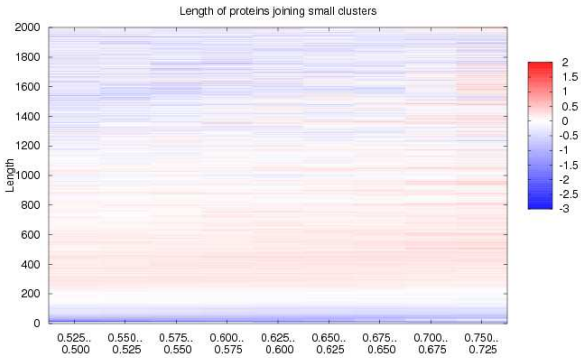

(a)

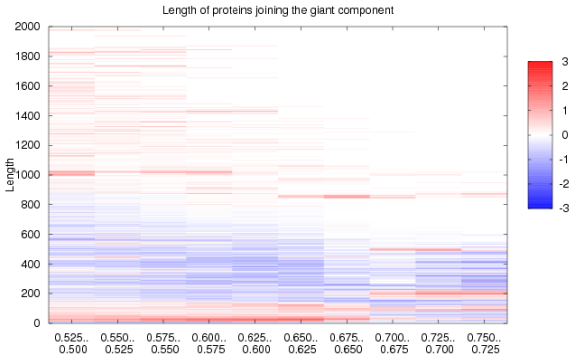

(b)

FIG. 10: Length representation of (a) proteins joining generic clusters and of (b) proteins joining the largest cluster. The red color encodes overrepresented lengths; the blue color indicates underrepresented lengths.

all SIMAP proteins.

For all weight intervals we have counted the feature occurrence in the proteins that connect clusters; these proteins are all pairs of sequences which belong to different clusters in the graph built at $\bar{w}_1$ and belonging to the same cluster in the graph built at $\bar{w}_2$, where $\bar{w}_2 < \bar{w}_1$ are two consecutive values of the weight $\bar{w}$. We have also distinguished between two disjoint sets of these proteins: proteins linking the clusters that will form the largest cluster in the graph built at $\bar{w}_2$ and proteins linking the other generic clusters.

The enrichment (e) of features was calculated as ratio of the number of features found (k) and the number of features expected (k_E): $e = k/k_E$. The number of features expected was calculated by: $k_E = K\,n/V$, where n is the number of proteins of interest (e.g. connecting clusters in a given weight interval), K denotes the number of proteins used for clustering having the given feature and V corresponds to the number of proteins used for clustering.

A. Results

Proteins joining clusters outside the largest cluster show an over-representation of lengths around 400aa (Figure 10(a)), contain overrepresented proteins of small low complexity content (Figure 11(a)), are often neutral or weakly acidic (Figure 12(a)) and contain more transmembrane proteins than expected (Figure 13(a)). Proteins joining clusters in the giant component are characterized by short and very long lengths (Figure 10(b)), reduced low complexity content (Figure 11(b)), acidic and alkaline proteins, dependent on the weight interval (Figure 12(b)) and a high number of transmembrane domains in the lower weight intervals (Figure 13(b)). Signal peptides were found overrepresented in proteins joining clusters outside the largest component at the lower weight intervals; at higher weight intervals and in proteins joining clusters in the largest component they were found underrepresented, as were localization sig-

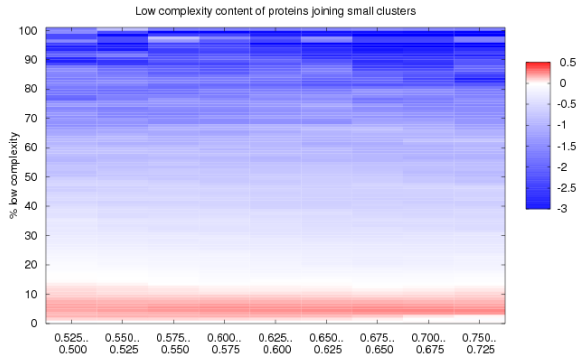

( )

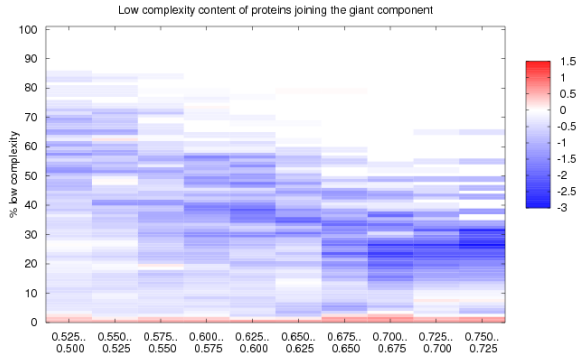

(b)

FIG. 11: Representation of the low complexity content of (a) proteins joining generic clusters and of (b) proteins joining the largest cluster. The red color encodes overrepresented values; the blue color indicates underrepresented values.

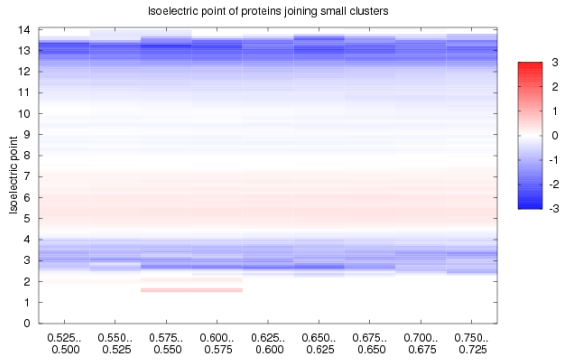

( )

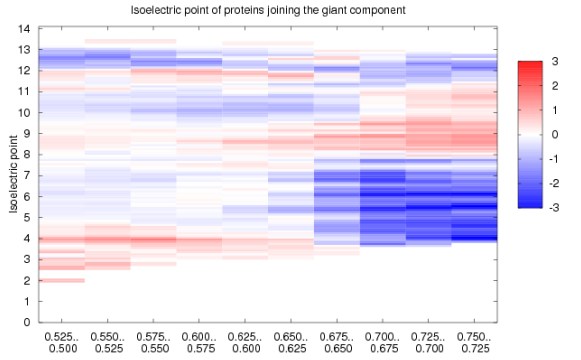

(b)

FIG. 12: Representation of the isoelectric points of (a) proteins joining generic clusters and of (b) proteins joining the largest cluster. The red color encodes overrepresented values; the blue color indicates underrepresented values.

nals in all proteins joining clusters (Figure 14(a) and Figure 14(b)). For all considered weight intervals we could find interval-specific overrepresented and underrepresented protein domains (Figure 15(a) and 15(b)). Remarkably these domains are not only specific for a certain weight interval, but also different for proteins joining clusters outside the largest component and proteins joining clusters in the largest component (See Table VI).

B. Discussion

All of the analyzed sequence features indicate that proteins that join clusters at a certain weight interval are not distributed equally over the complete protein space. For all of the features we could find specific under- and over-representation. Proteins joining clusters outside the largest component and proteins joining clusters in the largest component are different with respect to almost all considered features, which indicates that the largest component contains proteins that are different from those contained in other large clusters. These findings are complemented by the observation of specific over- and underrepresented functional domains in the proteins connecting clusters at certain weight intervals. Thus we conclude that for each weight interval a small number of protein families is responsible for cluster interconnections.

VIII. CONCLUSIONS

We investigated the local e global properties of the sequence similarity space formed by all proteins in the SIMAP database, which contains more than 5.5 millon amino acid sequences. We represented this space as a graph whose vertices are proteins and the edges are weighted to reflect the similarity between the corresponding pairs of sequences (high weight, high similarity). The choice of this weight formula (1) came from the

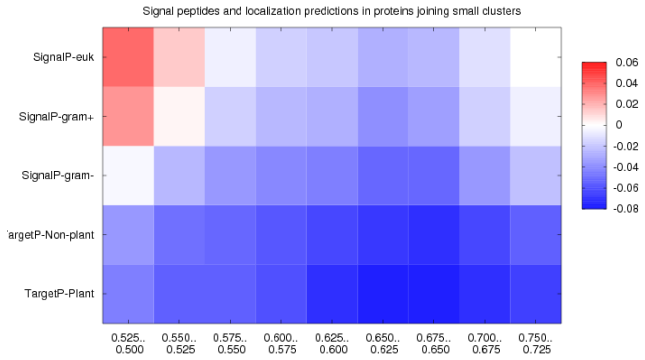

(a)

(a)

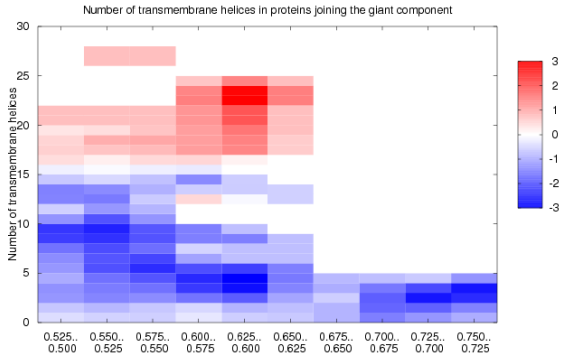

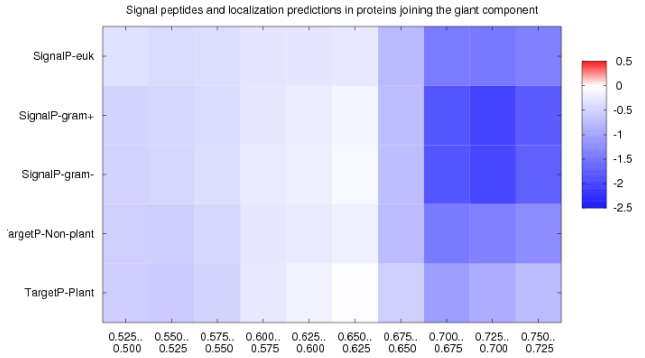

(b)

(b)

FIG. 13: Representation of the predicted number of transmembrane helices of (a) proteins joining generic clusters and of (b) proteins joining the largest cluster. The red color encodes overrepresented values; the blue color indicates underrepresented values.

FIG. 14: Representation of the predicted signal peptides and protein localization signals of (a) proteins joining generic clusters and of (b) proteins joining the largest cluster. The red color encodes overrepresented values; the blue color indicates underrepresented values.

necessity to compare the similarity score between pairs of sequences that could have different lengths. The SW score was therefore modified by means of the self-score geometric mean which contains the length information of the two aligned sequences.

Then, keeping only edges with $w \geq \bar{w}$, we built a collection of graphs by varing $\bar{w}$. From the analysis of the connected components we found that these graphs do not belong to the class of random graphs, whereas they are characterized by a power law behaviour both in the size cluster distribution and in the coordination degree distribution and for each fixed $\bar{w}$ these two distributions are strongly related to each other.

With the variation of $\bar{w}$, we found interesting changes in the global organization of the protein homology networks: we observed two different phases, one for large values of $\bar{w}$, characterized by the presence of clusters with similar dimensions, each composed essentially by proteins belonging to only one kingdom and with the largest one composed especially by viruses, and the second phase, for lower values of $\bar{w}$, characterized by the presence of a giant component composed by different species and other very little clusters.

In the end we investigated sequence features and functional informations of protein pairs that are responsible of the connection of clusters in the different intervals of $\bar{w}$, since they harbor the most conserved sequence regions that are shared by the interconnected clusters. We found that proteins joining clusters outside the largest component and proteins joining clusters in the largest component are different with respect to almost all considered features, which indicates that the largest component contains proteins that are different from those contained in other large clusters. Indeed we found an overrepresentation of a small set of domains which shows that a small number of protein families is responsible for cluster interconnections.

The analysis we performed gives a first view of the

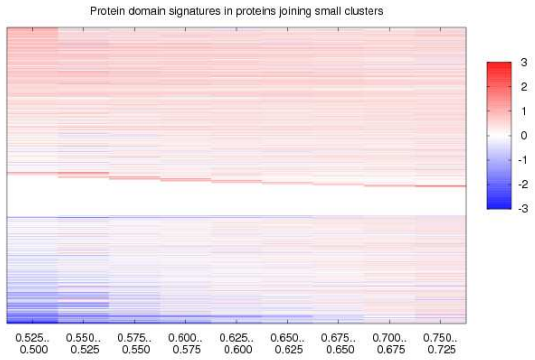

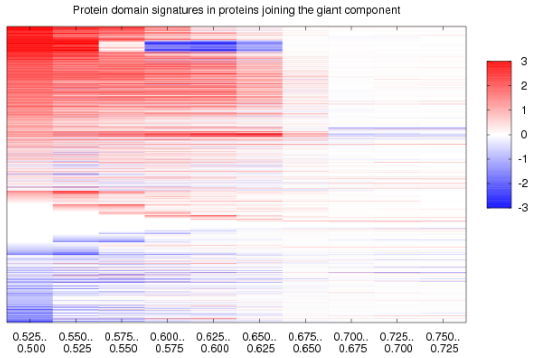

(b)

FIG. 15: Representation of the predicted protein domains of (a) proteins joining generic clusters and of (b) joining the largest cluster. Each line in the graph denotes a certain domain. The red color encodes overrepresented values; the blue color indicates underrepresented values.

global organization of the greatest protein homology network ever been built before. It is the first step and the starting point to answer to other global or local interesting questions which could confirm that the protein homology network is structured with respect to functional and evolutionary properties.

IX. ACKNOWLEDGEMENTS

The authors thanks Claudio Destri, Roland Arnold and Mattia Pelizzola for useful discussions, Michele Caselle for encouraging our collaboration and Patrick Tischler, Jan Krumsiek and Benedikt Wachinger for providing the software for protein feature calculation.

[1] E.V. Koonin, *Orthologs, Paralogs, and Evolutionary Genomics.*, Annu. Rev. Genet. 2005 39:309-38

[2] R. Arnold, T. Rattei, P. Tischler, M. Truong, V. Stümpflen, W. Mewes, *SIMAP - The similarity matrix of proteins*, Bioinformatics **21**, ii42-ii46 (2005)

[3] D. Medini, A. Covacci, C. Donati, *Protein homoloy network families reveal step-wise diversification of type III and type IV secretion systems.*, PLOS Computational Biology 2 1543-1551 (2006)

[4] P. Erdös, A. Rényi, *On random graphs*, I, Publ. Math. Debrecen **6**, 290-291 (1959)

[5] L. Bogacz, Z. Burda, W. Janke, B. Waclaw, *A program generanting homogeneous random graph with given weights*, [cond-mat/0506330].

[6] P. Rice, I. Longden, et al., *EMBOSS: the European Molecular Biology Open Software Suite*, Trends Genet 16(6): 276-7 (2000)

[7] J.C. Wootton, *Sequences with 'unusual' amino acid compositions.*, Curr. Opin. Struct. Biol 4: 413-421 (1994)

[8] A. Krogh, B. Larsson, et al., *Predicting transmembrane protein topology with a hidden Markov model: application to complete genomes.* , J. Mol. Biol 305(3): 567-580 (2001)

[9] J.D. Bendtsen, H. Nielsen, et al., *Improved prediction of signal peptides: SignalP 3.0.* , Journal of Molecular Biology 340(4): 783-795 (2004)

[10] O. Emanuelsson, H. Nielsen, et al., *Predicting subcellular localization of proteins based on their N-terminal amino acid sequence.*, Journal of Molecular Biology 300(4): 1005-1016 (2000)

[11] N.J. Mulder, R. Apweiler, et al., *InterPro, progress and status in 2005.*, Nucleic Acids Research 33 (Database issue): D201-5 (2005)

[12] Due to duplication and shuffling of coding segments in the akno DNA during the evolution.

[13] For simplicity we will use the same notation to point graphs's nodes and database's proteins.

$\bar{w}_1 \rightarrow \bar{w}_2$	e	Proteins joining generic clusters	e	Proteins joining the largest cluster
	0.02	PF00598 Flu_M1	0.93	PF00078 RVT_1
	0.03	PF00522 VPR	1.08	PF00075 RnaseH
	0.03	PF00540 Gag_p17	1.44	PF06815 RVT_connect
	0.03	PF00951 Arteri_Gl	1.46	PF07075 DUF1343
	0.03	PF00971 EIAV_GP90	2.19	PF00665 rve
0.750 → 0.725				
	9.40	PF02916 DNA_PPF	15.41	PF00607 Gag_p24
	11.09	PF07095 IgaA	18.79	PF00517 GP41
	11.25	PF08272 Topo_Zn_Ribbon	18.91	PF02022 Integrase_Zn
	11.83	PF06899 WzyE	27.07	PF00540 Gag_p17
	12.46	PF06788 UPF0257	137.49	PF00516 GP120
			0.88	PF00078 RVT_1
			1.16	PF00077 RVP
			1.91	PF06817 RVT_thumb
			3.68	PF00075 RnaseH
			3.77	PF00665 rve
0.725 → 0.700				
			37.19	PF00186 DHFR_1
			80.26	PF00098 zf-CCHC
			129.77	PF00516 GP120
			139.92	PF00607 Gag_p24
			145.50	PF00540 Gag_p17
	0.01	PF00516 GP120	0.12	PF00098 zf-CCHC
	0.01	PF00522 VPR	0.15	PF00271 Helicase_C
	0.01	PF00602 Flu_PB1	0.22	PF00078 RVT_1
	0.01	PF00603 Flu_PA	1.02	PF01560 HCV_NS1
	0.01	PF01539 HCV_env	1.16	PF06817 RVT_thumb
0.700 → 0.675				
	10.14	PF08435 Calici_coat_C	15.62	PF02907 Peptidase_S29
	10.22	PF03296 Pox_polyA_pol	19.47	PF00517 GP41
	12.94	PF05733 Tenui_N	57.66	PF00516 GP120
	12.98	PF03805 CLAG	74.03	PF00077 RVP
	13.68	PF00897 Orbi_VP7	98.38	PF02348 CTP_transf_3
	0.01	PF00064 Neur	0.10	PF00078 RVT_1
	0.01	PF00469 F-protein	0.13	PF00077 RVP
	0.01	PF00506 Flu_NP	0.18	PF00560 LRR_1
	0.01	PF00516 GP120	0.18	PF00607 Gag_p24
	0.01	PF00540 Gag_p17	0.30	PF00665 rve
0.675 → 0.650				
	11.63	PF04310 MukB	151.92	PF02959 Tax
	12.71	PF07108 PipA	168.64	PF00758 EPO_TPO
	13.48	PF07429 Fuc4NAc_transf	431.37	PF08300 HCV_NS5a_1
	15.20	PF03506 Flu_C_NS1	441.03	PF08301 HCV_NS5a_1b
	15.26	PF06593 RBDV_coat	483.96	PF01506 HCV_NS5a
	0.01	PF00506 Flu_NP	0.03	PF00096 zf-C2H2
	0.01	PF00516 GP120	0.04	PF00078 RVT_1
	0.01	PF00540 Gag_p17	0.17	PF00023 Ank
	0.01	PF00603 Flu_PA	0.17	PF00589 Phage_integrase
	0.01	PF00695 vMSA	0.19	PF00903 Glyoxalase
0.650 → 0.625				
	12.57	PF06952 PsiA	202.08	PF01002 Flavi_NS2B
	13.73	PF06788 UPF0257	221.93	PF01349 Flavi_NS4B
	14.79	PF05788 Orbi_VP1	222.59	PF01353 GFP
	15.42	PF00901 Orbi_VP5	229.23	PF01350 Flavi_NS4A
	16.02	PF03753 HHV6-IE	243.38	PF00948 Flavi_NS1

[14] These sequences come from databases: *PDB proteins*, *mips non-redundant protein database*, *UNIPROT SWISSPROT*, *UNIPROT-TrEMBL*, *PFAM sequences*, *Eukaryotic signature proteins*.

[15] The values for background distribution of amino acids come from data used for the PAM matrix: $p_A = 0.096$; $p_R = 0.034$; $p_N = 0.042$; $p_D = 0.053$; $p_C = 0.025$; $p_Q = 0.032$; $p_E = 0.053$; $p_G = 0.090$; $p_H =$

	0.01	PF00124 Photo_RC	0.09	PF00009 GTP_EFTU
	0.01	PF00603 Flu_PA	0.13	PF07974 EGF_2
	0.01	PF00695 vMSA	0.2	PF00096 zf-C2H2
	0.01	PF01560 HCV_NS1	0.22	PF00560 LRR_1
	0.02	PF00223 PsaA_PsaB	0.23	PF01546 Peptidase_M20
$0.625 \rightarrow 0.600$				
	11.95	PF06517 Orthopox_A43R	376.41	PF01002 Flavi_NS2B
	12.09	PF00843 Arena_nucleocap	403.70	PF00948 Flavi_NS1
	13.08	PF06802 DUF1231	411.72	PF01349 Flavi_NS4B
	14.72	PF05273 Pox_RNA_Pol_22	425.27	PF01350 Flavi_NS4A
	16.90	PF03021 CM2	538.21	PF05408 Peptidase_C28
	0.01	PF00517 GP41	0.06	PF00096 zf-C2H2
	0.01	PF00559 Vif	0.06	PF00097 zf-C3HC4
	0.01	PF00600 Flu_NS1	0.09	PF00009 GTP_EFTU
	0.01	PF00969 MHC_II_beta	0.09	PF01266 DAO
	0.01	PF06815 RVT_connect	0.11	PF01926 MMR_HSR1
$0.600 \rightarrow 0.575$				
	10.54	PF02477 Nairo_nucleo	133.87	PF05790 C2-set
	11.95	PF07982 Herpes_UL74	139.12	PF01353 GFP
	12.30	PF06871 TraH_2	150.11	PF00518 E6
	14.14	PF02509 Rota_NS35	195.29	PF02929 Bgal_small_N
	16.04	PF06929 Rotavirus_VP3	231.71	PF01382 Avidin
	0.01	PF00016 RuBisCO_large	0.02	PF00115 COX1
	0.01	PF00113 Enolase_C	0.07	PF07690 MFS_1
	0.01	PF00123 Hormone_2	0.08	PF07993 NAD_binding_4
	0.01	PF00506 Flu_NP	0.09	PF00517 GP41
	0.01	PF01010 Oxidored_q1_C	0.10	PF00583 Acetyltransf_1
$0.575 \rightarrow 0.550$				
	10.60	PF06134 RhaA	161.43	PF01140 Gag_MA
	10.95	PF07095 IgaA	168.19	PF04528 Adeno_E4_34
	11.75	PF00897 Orbi_VP7	173.44	PF08377 MAP2_projctn
	12.13	PF03294 Pox_Rap94	184.23	PF02093 Gag_p30
	13.75	PF01295 Adenylate_cycl	311.32	PF01141 Gag_p12
	0.01	PF00016 RuBisCO_large	0.06	PF00067 p450
	0.01	PF00516 GP120	0.07	PF00023 Ank
	0.01	PF00522 VPR	0.08	PF00097 zf-C3HC4
	0.01	PF00540 Gag_p17	0.11	PF01381 HTH_3
	0.01	PF01539 HCV_env	0.11	PF04851 ResIII
$0.550 \rightarrow 0.525$				
	11.29	PF05928 Zea_mays_MuDR	101.41	PF01537 Herpes_glycop_D
	11.62	PF06829 DUF1238	121.18	PF02929 Bgal_small_N
	11.63	PF03277 Herpes_UL4	123.25	PF01376 Enterotoxin_b
	11.64	PF03395 Pox_P4A	128.24	PF06466 PCAF_N
	12.73	PF08405 Calici_PP_N	147.36	PF05806 Noggin
	0.01	PF00600 Flu_NS1	0.02	PF00106 adh_short
	0.01	PF00869 Flavi_glycoprot	0.04	PF00270 DEAD
	0.01	PF01539 HCV_env	0.05	PF00037 Fer4
	0.01	PF02461 AMO	0.06	PF02518 HATPase_c
	0.01	PF02788 RuBisCO_large_N	0.08	PF00249 Myb_DNA-binding
$0.525 \rightarrow 0.500$				
	11.36	PF07434 CblD	68.92	PF03939 Ribosomal_L23eN
	11.80	PF04913 Baculo_Y142	72.11	PF06267 DUF1028
	11.98	PF05880 Fiji_64_capsid	96.66	PF02022 Integrase_Zn
	13.48	PF06306 CgtA	120.34	PF00552 Integrase
	13.98	PF03317 ELF	129.98	PF02929 Bgal_small_N

TABLE VI: For proteins joining clusters outside the largest component or joining the giant component the five mostly underrepresented and five mostly overrepresented PFAM domains are giver per interval of weight w.

0.034; $p_I = 0.035$; $p_L = 0.084$; $p_K = 0.085$; $p_M = 0.012$; $p_F = 0.045$; $p_P = 0.041$; $p_S = 0.057$; $p_T = 0.062$; $p_W = 0.012$; $p_Y = 0.030$; $p_V = 0.078$.

They can be obtained from *http://apps.bioneq.qc.ca/twiki/pub/Knowledgebase/PAM/PAM2.JPG*